J Ther Eng, Vol. 10, No. 5, pp. 1306−1322, September, 2024

Journal of Thermal Engineering
Web page info: https://jten.yildiz.edu.tr
DOI: 10.14744/thermal.0000870

Research Article

Investigation of a standard gate valve in terms of flow rate, opening distance and wedge angle with CFD

Soner ENEKCİ[1,*], Usame DEMİR[2], Kadir YILMAZ[1]

[1]*Department of Energy Systems Engineering, Kocaeli University, Kocaeli, 41380, Türkiye*
[2]*Department of Mechanical Engineering, Bilecik Seyh Edebali University, Bilecik, 11230, Türkiye*

ARTICLE INFO

Article history
Received: 04 December 2022
Revised: 13 March 2023
Accepted: 13 March 2023

Keywords:
CFD Analysis; Gate Valve; Pressure Drop; Wedge Angle

ABSTRACT

Gate valves provide sealing with metal-to-metal friction. When the right interior parts are selected, and the production is not made according to the proper design criteria, internal leaks occur in the valves in the medium term. Considering the ideal pressure, velocity equations and designs suitable for the process can be realized by determining the nominal pressure and velocity curves. This study designed a standard gate valve with 8-inch connection dimensions. Computational Fluid Dynamics (CFD) method investigated split, flexible, and solid wedge types of the designed valve, 0.5, 1, and 2 m/s flow velocities for zero, four and five-degree wedge closing angles and 20 mm, 40 mm, 60 mm, 90 mm, and 120 mm opening wedge positions. Ansys Fluent software was used for the analyses. Mesh optimization was performed for the ideal mesh number and analyzed according to the ideal mesh number. The k-Epsilon turbulence model was used for simulations. The same situations were repeated for a parallel wedge (0-degree wedge seating angle). The lowest pressure distribution and pressure loss occurred in the parallel wedge compared to the opening position of other types of wedges. The best gate type obtained from the analysis results was determined, and an experimental tightness test was performed. It can be said that the soft seat gate valve, designed according to the results of the sealing test, gives approximately 2.5 times more opening-closing life than the metal gate valve, thus reducing the maintenance-repair costs.

Cite this article as: Enekci S, Demir U, Yilmaz K. Investigation of a standard gate valve in terms of flow rate, opening distance and wedge angle with CFD. J Ther Eng 2024;10(5):1306−1322.

INTRODUCTION

Recently, valves have been used to control fluids [1]. These valves have different features and characteristics depending on the sector or fluid type [2]. All valves used in pipelines of filling facilities must have a long service life [3]. Technical features such as opening and closing of valves at low torque values and providing superior sealing are required [4]. These features cannot be met with standard products. The wedge type and wedge closing angle are critical factors that influence the performance and lifespan of valves [5]. The wedge type determines the amount of force required to close the valve, affecting its durability and ease of operation [6]. A flexible wedge, for example, is

*Corresponding author.
*E-mail address: sonerenekci@gmail.com

This paper was recommended for publication in revised form by Associate Editor Erman Aslan

more durable and can handle thermal expansion and contraction better than a solid wedge [7]. The wedge closing angle affects the stress and wears on the valve components during operation. A larger closing angle can result in more stress and wear on the valve components, reducing lifespan. Therefore, selecting the appropriate wedge type and closing angle is crucial in ensuring valves' optimal performance and longevity [8].

Many studies are carried out in the industry to provide the features above. Some of these studies focus on structural solutions, while others suggest usability improvements. In this context, the studies conducted in the literature are briefly summarized below;

Tverskoy et al. [9] expressed analog actuators with aspherical construction for double-gate shut-off and controlled spherical valves had proven to provide outstanding technical characteristics (bandwidth and control range) compared to analog actuators. They suggested that these valves could be used especially in tankers and fire trucks due to the double closing and controlled spherical valve types being more functional and occupying less space. In another study, Zakirnichnaya and Kulsharipov [10] examined the feasibility of a longer-life design of wedge-type gate valves. Flow-structural analysis solutions with the FLOWVISION software, analyzes were carried out for the change in the operating parameters of wedge gate valves, such as medium density, viscosity, temperature, pressure and fluid velocity, and lifetime. It was revealed that the increase in pressure and fluid velocity from these parameters caused the normal maintenance periods of wedge-type gate valves to be shortened. The main inlet valve of the thermal power plant operating with the steam cycle made of steel with a martensite structure has been studied. They are evaluated in terms of strength and service interval and life. They tested the inlet valve made of martensite steel material for 170,000 hours in a thermal power plant with operating conditions of 545 °C and 19 MPa. After the test, the valve was removed and comprehensive microstructural analysis, examination of the microstructure on the surface and in the wall, and thickness were performed. According to the results obtained, they observed changes in impact toughness, while the microstructural deterioration caused by long-term operation had little effect on the hardness and strength of the material [11]. Tripathy et al. [12] carried out the development of the electro-pneumatic valve for the camless engine. In this case, they studied that the valve's fast closing caused some problems; therefore, the valve could be closed properly by controlling its speed. It has been shown that when the valve is closed with a speed of 1 m/s, the valve is closed very well on the seating surface and the sealing is provided well. Ethylene Propylene Diene Monomer (EPDM) O-rings gate valves used in the production of a 2nd gen accelerator of Neutron Rich Radioactive Ion Beams were examined to evaluate their sealing performance during both plant service life and after-service storage. Several tests evaluated the corresponding modifications of materials' properties. These evaluations determined a life estimation schedule as service and storage time and O-ring tightening degree [13]. Kim et al. [14,15] in their study; analyzed the effects of differential pressure changes on the friction coefficient. They determined the limit value of the body friction coefficient. They obtained by analyzing the experimental results that the fluid pressure affected the body friction coefficient at medium and high differential pressure, but the body friction coefficient at low differential pressure was almost not affected by the fluid pressure. Valve analysis was performed by designing a total of 49 different parameters, including valve size, shaft size, actuator model, lubricant test, and loading speeds. According to the valve test results, the loading speed appeared to increase as the pressure difference increased and under high differential pressure .Teodoro and Moutinho [16] in their study, designed a compact slide valve for the ultra-high vacuum system. The valve is designed to isolate an ion gun used in a surface analysis system. Routine maintenance of the Ion supply using a compact gate valve has saved approximately 2 days of pumping and superheating the entire system. Quin et al. studied three different valve types experimentally. The first study investigated Pilot Controlled Spherical Valve (PCSV). To open and close the main valve with a small pilot valve, they have implemented a design that can use the pressure difference caused by the fluid flow through the hole on the valve core as power. Analysis results showed that higher inlet velocity could lead to larger pressure difference with fast reply and PCSV wasn't suitable for low-velocity flow pipelines. They were also analyzed using the renormalization group k-$\mathcal{E}$ turbulence model and UDF and dynamic mesh renewal methods in Ansys Fluent software, which can perform both experimental and CFD for pilot-controlled globe valves. According to the analysis results obtained, five different equations were proposed for spring stiffness, and the equation that gave the closest spring stiffness value to the experimental results was proposed [17–19]. Alimonti [20] carried out experiments for single-phase and dual-phase flow for DN 200 spherical and gate valves and investigated pressure drops in dual-phase flow. As a result, they determined that the homogeneous equivalence model was the model that best predicted the pressure drop. Paolinelli et al. [21] studied the sizes of water droplets produced by the passage of oil-water flow through a ball valve placed in a large-scale flow loop with an inside diameter of 0.1 m. The experiments were carried out under different pressure drops and different oil and water flow rates across the ball valve. Another ball valve study conducted a simulation study to examine the aeroacoustics of the ball control valve. Numerical analyzes were made using the axially symmetrical globe control valve (2.54 cm), 2-dimensional large eddy simulation for different valve openings, and Large Vortex Simulation turbulence model. Ffowcs-Williams and Hawkings (FWH) models were used to model aero-acoustics. Of these modifications, the 20° chamfer on the valve

seat inlet side showed the lowest sound pressure level for the various openings of the ball control valve [22].

Mitrovic et al. [23] used System Aramis based on the Digital Image Correlation method for experimental and numerical model validation. The complex structure studied is the ball/cylinder connection point on the spherical valve body subjected to axial load. In this way, they proved that the results for Digital Image Correlation and Finite Element Method are sufficient and the methods are mutually valid. Ferrari and Leutwyler's experimental and simulation studies were carried out for cavitation condition, flow rate, and disc position on a 2" ball valve. In the experimental study, they revealed that cavitation did not have a serious effect on the transfer force. The maximum transversal force was obtained at mid-span (between 6 and 10 mm) and they could reach 25% of the maximum axial force. The numerical estimates were verified experimentally and they provided a better approach to the force caused by the flow on the body [24]. A new valve mechanism with a six-bar linkage operating mechanism has been proposed to reduce the valve height by replacing the piston rod. Analyzes of the mechanism were made using 3D-CAD software. Numerical analysis was performed using software for mechanism, force, positioning, and flow analysis. Flow analysis of the valve, on the other hand, showed that the new mechanism was a failed attempt [25]. Lin et al. carried out the Computational Fluid Dynamics- Discrete Element Method (CFD-DEM) simulation method is adapted to study the gas-solid two-phase flow properties and erosion properties of the gate valve. According to the results obtained, particle distribution showed that the number of particles in front of the overflow cap increased with decreasing valve opening [26]. Hu et al. investigated the heat transfer of the underwater gate valve with the 3D constant of The Reynolds-averaged Navier-Stokes (RANS) method and simulation with the Computational Fluid Dynamics software ANSYS ICEM. According to the results obtained, it was revealed that the distribution of temperature and convection heat transfer coefficient was different in the upwind and downwind surfaces in the flow area. They also determined that Low Reynolds Number Modeling gave more accurate results than the Wall Function model [27]. Borooghani et al. [28] were presented and evaluated a moral failure of a gate valve cover in pit top installations. After about 48,240 hours of service in acidic gas, a crack was found in the body. They suggested annealing as heat treatment to reduce shell crack susceptibility, reduce hardness, and prevent premature failure. In the literature, it has been seen that many studies have been carried out with finite element method analysis [29–32] and computational fluid dynamics method [33–41] in general. It can be said that the number of studies on the gate valve is very few.

Valves are essential components in various industries, including oil and gas, power generation, water treatment, and chemical processing. They are responsible for controlling the flow of liquids and gases through pipelines and other systems. The performance and lifespan of a valve depend on several factors, including the wedge type and the wedge closing angle. The wedge type refers to the shape of the wedge that moves up and down to open and close the valve. The wedge is typically made of metal, and its design affects the amount of force required to close the valve. The wedge type also influences the valve's durability and ease of operation. One type of wedge is the solid wedge, a single piece of metal that tapers toward the bottom. It is simple in design and easy to manufacture but can be prone to sticking due to thermal expansion and contraction. The solid wedge can also cause turbulence in the flow of fluids, leading to erosion and corrosion. The flexible wedge, on the other hand, is more durable and can handle thermal expansion and contraction better. It has a split design allows it to bend slightly under pressure, reducing the likelihood of sticking. The flexible wedge also creates a more streamlined flow, reducing turbulence and erosion. The wedge closing angle is another critical factor that affects the lifespan and operation of valves. When the valve is closed, an angle is formed between the wedge and the valve seat. A larger closing angle can result in more stress and wear on the valve components during operation, reducing lifespan. For example, a wedge with a 60-degree closing angle will exert more force on the valve seat than a 30-degree closing angle. This additional force can cause wear and damage to the valve components over time, leading to leaks and other issues. In summary, selecting the appropriate wedge type and wedge closing angle is crucial in ensuring the optimal performance and longevity of valves. The flexible wedge is generally more durable and better at reducing turbulence than the solid wedge, while a smaller closing angle can help reduce stress and wear on the valve components

In this study, as seen in the literature, there is no study on gate valve types, especially according to the wedge type and wedge closing angle. Analyses were performed and evaluated for the gate valve according to three different wedge angles and types and five different wedge opening positions.

MATERIALS AND METHODS

Cfd Study

Gate-type valve applied to oil transportation system is mainly studied in this paper. The working way of a gate valve is: valve stem drives gate opening and closing. There are three commonly used gate forms: straight panel-type gate, hollow straight panel-type gate, and wedge-shaped gate. The most proper gate type (Wedge-shaped gate valve) should be selected according to fluid characteristics for oil transportation. For wedge-type gate valves, wedge shapes are important for sealing.

The gate valve shaft moves with the gate, which is the sealing part. It provides linear ascending and descending functions on the Y-axis. The sealing part contacts the

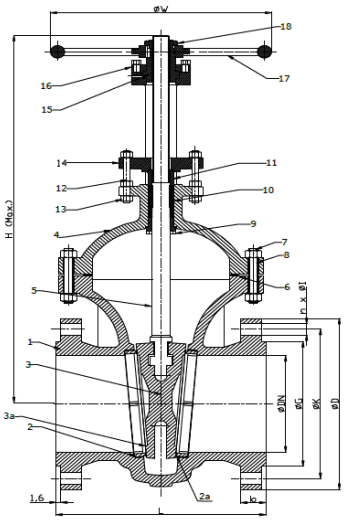

1-BODY
2-SEAT
3- WEDGE
4- BONNET
5- STEM
6- GASKET
7- NUT
8- STUD BOLT
9- BACK RING
10-PACKING
11-GLAND
12-STUD BOLT
13-NUT
14-GLAND FLANGE
15- STEM BUSHING
16- BUSHING NUT
17- HANDWELL
18-HANDWELL NUT

Figure 1. Standart gate valve partition list and dimensions.

surface of the valve body and provides full sealing. It is provided by metal contact between sealing surfaces or high-strength Teflon materials. In our design, Teflon is mounted on the metal to cover the contacting surfaces on the sealing part, and the sealing surface is soft and highly impermeable. In this study, the gate valve dimensions, whose geometrical details are given, were determined in accordance with the standards given by the International American Petroleum Institute. The technical details of a designed gate valve are shown in Figure 1.

Table 1. Dimensions of the gate valve used

DIMENSIONS									
ØDN mm	ØD mm	b mm	ØG mm	ØK mm	n	ØI mm	L mm	H mm	ØW mm
8”	343	29	270	299	8	22	292	1035	415

In addition, the basic dimensions in the geometry given in Figure 1 are given in Table 1. ØDN indicates the nominal diameter of the valve. ØD is the flange diameter, ØK is the diameter between the stud axes, ØG is the gasket surface diameter, b is the flange wall thickness, L is the distance between the two flanges, H is the height of the valve from the flow axis line, ØW is the handwell dimension diameter.

This study investigated the effects of wedge closing angle, wedge type, and wedge lift height, especially for wedge-type gate valves. The technical details of different wedge closing angles for the 8-inch wedge-type valve are shown in Figure 2. A standard-type gate valve wedge design with 0, 4, and 5-degree wedge angles are given with a section view. The CAD model of this new design was created in Solidworks software. Simulation studies have been carried out for different wedge closing angles and types. Flow analyses were carried out with Ansys Fluent 19.0. All necessary equipment of a standard type gate valve, whose analysis has been completed successfully.

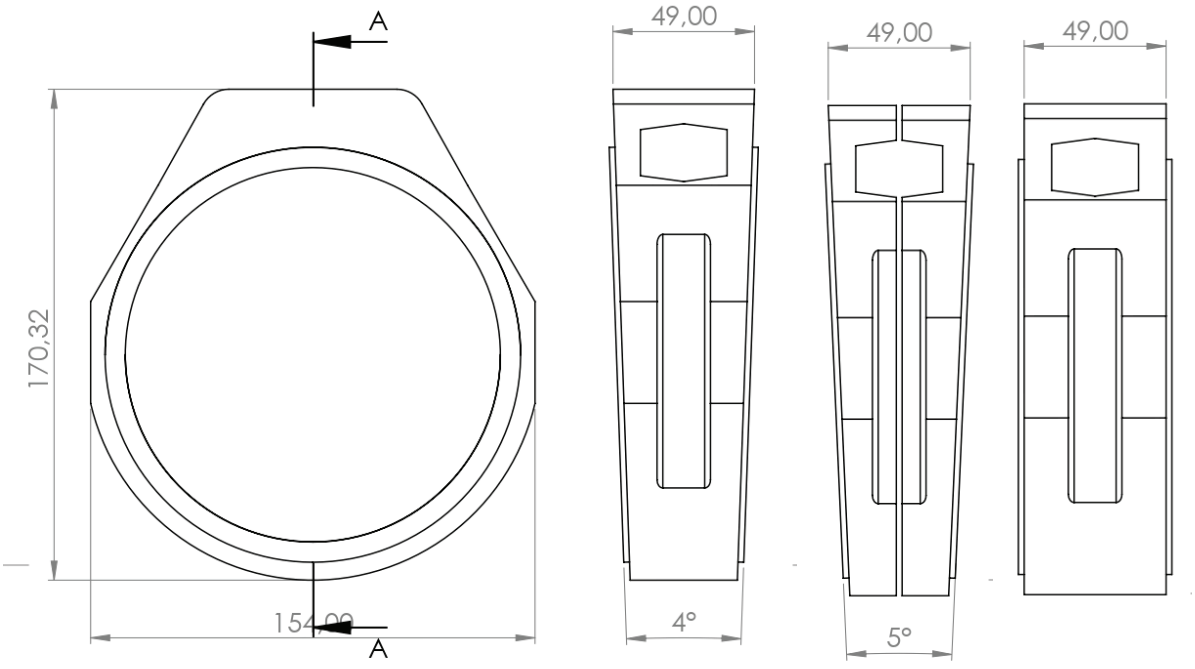

Figure 2. Type of gate valve wedge section view.

For simulation, it is necessary to define physical parameters for a given numerical model/submodel, including the definition of the input variables and their values, the definition of a model type, the definition of the dynamic and kinematic viscosity, and the initial and boundary conditions. A single-phase problem is selected, meaning only one fluid is defined in the problem (water at 25°C). A stationary flow regime with a reference pressure of 101,325 Pa without heat transfer within the model and the so-called k–ε turbulence model with standard wall function was chosen for the simulation. The first variable (k) represents the turbulent kinetic energy and the second transport variable (ε) refers to the dissipation rate of the turbulent kinetic energy. The transport equation for k is described by the expression (1) and the transport equation for ε by the expression (2) [42]

$$\rho \frac{D_k}{D_t} = \mu_t \left(\frac{\partial U_j}{\partial x_i} + \frac{\partial U_i}{\partial x_j} \right) \frac{\partial U_j}{\partial x_i} + + \frac{\partial}{\partial x_i} \left\{ (\mu + \mu_t / \sigma k) \frac{\partial k}{\partial x_i} \right\} - \rho\varepsilon + G_b - Y_m + S_k \quad (1)$$

$$\rho \frac{D\varepsilon}{Dt} = C_{1\varepsilon} \left(\frac{\epsilon}{k} \right) \left[\mu_t \left(\frac{\partial U_j}{\partial x_i} + \frac{\partial U_i}{\partial x_j} \right) \frac{\partial U_j}{\partial x_i} + C_{3\varepsilon} G_b \right] + \frac{\partial}{\partial x_i} \left\{ (\mu + \mu_t / \sigma k) \frac{\partial \varepsilon}{\partial x_i} \right\} - C_2 \varepsilon \rho \left(\frac{\varepsilon^2}{k} \right) + S_\varepsilon \quad (2)$$

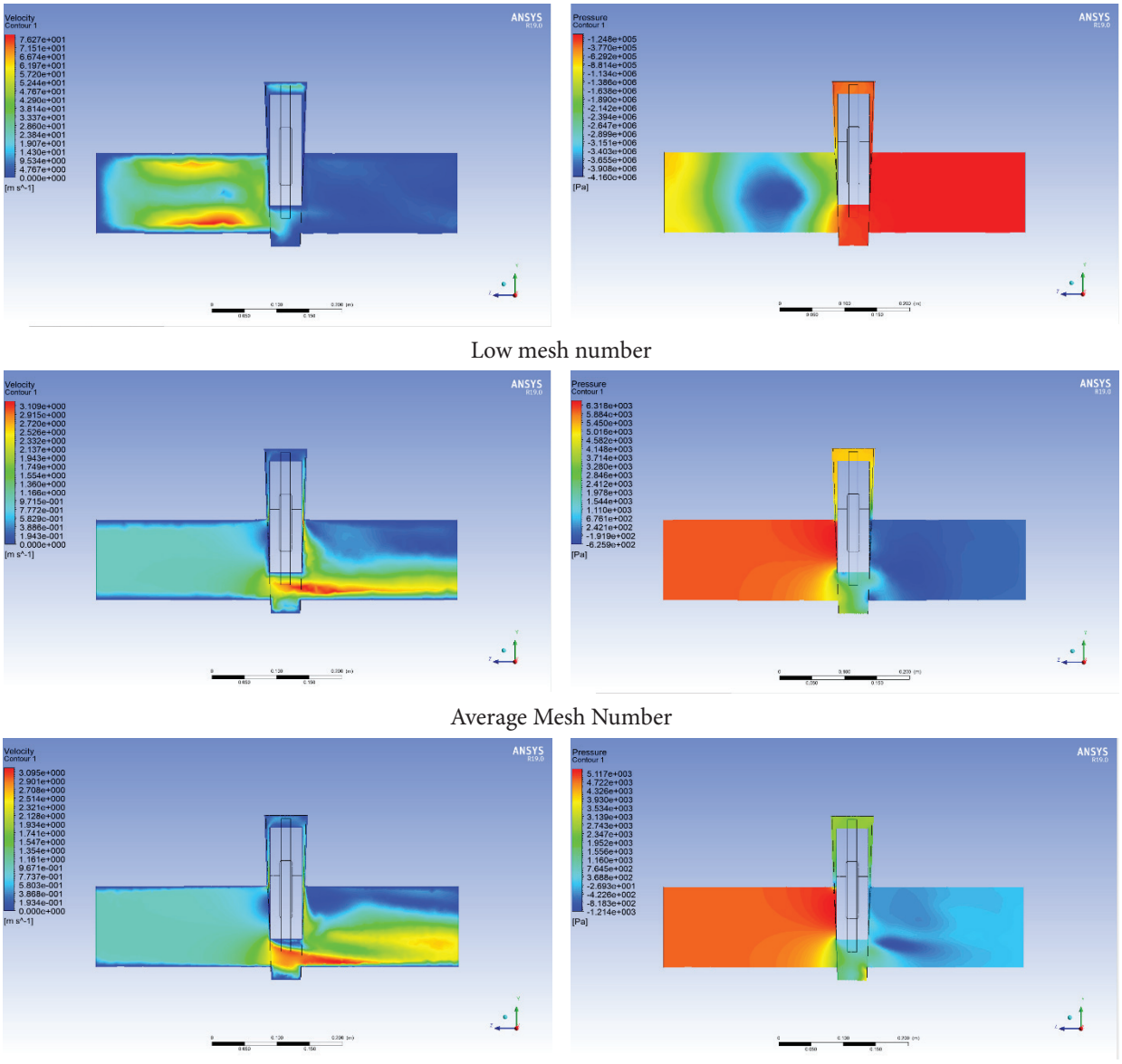

Figure 3. Mesh independency for solid wedge simulation at one m/s flow.

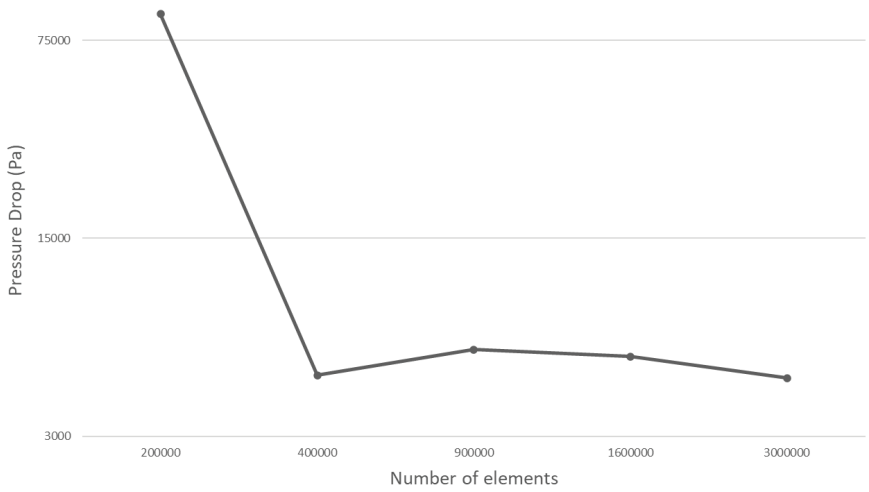

Figure 4. Mesh independence for the relationship between the pressure drop and the number of elements.

It has been tested in 3 different numbers Low mesh number (326700), Average Mesh number (average 1100000), and High Mesh number (approximately 300000) mesh number. Figure 2 shows the velocity and pressure distributions of the analyses performed at a flow rate of 1 m/s for the solid wedge type for mesh independence. As can be seen from the figure, it is seen that the velocity and pressure distributions for the average mesh number, i.e., 1.1 million mesh number and 3 million mesh number, show a similar situation. For this reason, approximately 1.1 million mesh numbers were used for all analyses. The result of the mesh independency related to pressure drop is also given in Figure 4. As seen in the graph, it was seen that the mesh number did not affect the result after approximately 500 thousand mesh count. For this reason, 1.1 million mesh numbers were used in the analysis. This is seen in both DP and velocity contour images.

CAD Model imported directly into ANSYS Workbench Design Modeler as a STEP file. Fluid volume is created using the Design Modeler Fill operation and converting Inlet and Outlet surfaces. Meshing was performed using the Fluent method available within the framework of the ANSYS mesh generator. Optimizing the mesh numbers allows the mesh to have 1.1 million tetrahedron elements for all cases. It was seen that the mesh structure affected the results at a lower mesh number. Larger mesh numbers could not be used because it forced the computer capacity. Application of tetrahedral elements for internal regions meshing allowed automatic mesh generation. Advanced sizing functions were used with automatic mesh inflation depending on wall proximity and curvature. Figure 5 shows the mesh structure.

A finite element formulation based on a SIMPLE-type algorithm was adopted to solve the incompressible Navier-Stokes equations. Also, the main difference between the first and second order is the number of points used for the computation, i.e., one upstream point for the first order and two for the second order. Usually, it is better to use the second-order scheme. Second-order upwind is used for simulation. Hybrid initialization should be preferred and usually, it accelerates the overall computation. Standard initialization is just filling the filed properties with constant values, while hybrid initialization solves several iterations (10) of a simplified equation system and thereby usually gets a better guess for the flow variables, particularly the pressure field.

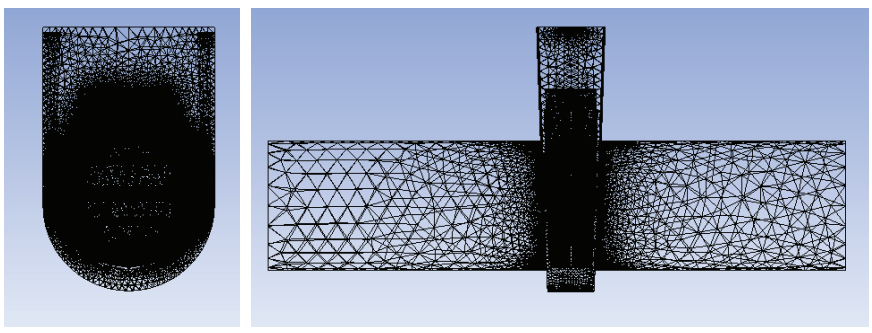

Figure 5. CFD mesh model of gate valve.

Figure 6. Experimental setup.

Experimental Test

It is aimed to extend the sealing life by strengthening the sealing equipment of a standard gate valve with an 8" connection size and 150 Class Pressure class, based on the opening and closing times. Special sealing equipment is placed in the channel made on the same wedge. PTFE-type Teflon sealing equipment is used. Two different valves were subjected to a 22-bar test and a three-minute test period in the same test setup, meeting API 600 gate valve standards. The test application was performed by performing each valve's opening and closing 100 times and retesting. Each test result was observed after 100 opening and closing counts. The number of first leaks was calculated with the help of this mechanism. Figure 6 shows the visuals of the experimental setup and the images of the tested gate valves.

In order not to change the valve control torque values, manual opening, and closing is not done. An electric actuator is used, which is mounted on the valve and will automatically open and close the valve.

A minimum of 30% more torque than the calculated torque value is required for the valve.

The actuator is electrically driven and the actuator supply is 220 VAC ± 10% and 50 Hz and mounted on the valve.

The actuator has a minimum of 4 digital inputs in the Control Unit. These digital inputs are individually set as open, close, stop, and emergency.

On/off operations are performed via the Control Unit. Valve Opening and closing times are 2 minutes.

RESULTS AND DISCUSSION

CFD Results

4° and 5° closing angles for flexible solid and split wedge types of the modeled standard type valve and 0.5 m/s, 1 m/s, and 2 m/s fluid velocities at 20 mm, 40 mm, 60 mm, 90 mm, and 120 mm wedge openings for the analysis, the results of the pressure distribution analysis were examined. For the analysis, the boundary conditions were adjusted according to these values and the results were obtained.

Figure 7 shows pressure distributions of 20 mm wedge opening and 4 degrees wedge closing angle. In general, it is understood that the pressure in the inlet part is higher than in the outlet part. Especially when looking at the split wedge, it can be said that there is more pressure in the middle of the wedge than in other types of wedges, which may cause pressure loss in the flow and the wedge should be specially coated since it is exposed to drag pressure for the wedge. It is seen that a split wedge occurs for maximum regional pressure of 0.32 MPa and a flow rate of 2 m/s. With the increase in flow rate, it is seen that pressure builds up on the left wedge surface at the 20 mm opening position of the valve at the inlet.

Figure 8 shows 40 mm wedge opening and 4 degrees wedge closing angle pressure distributions. It is seen that a similar situation occurs according to the 20 mm opening position. However, it is understood that the pressure

distribution is especially higher at low speeds at the wedge exit section, where the pressure is higher at the wedge tip than at the 20 mm opening position. It is seen that the pressure in the split wedge type is higher than in other wedge types. With the flow velocity increasing from 0.5 m/s to 2 m/s for the 40 mm wedge opening, the maximum pressure formed due to the analysis increased approximately 16.3, 16.2, and 15.67 times for flexible, solid and split wedge types, respectively. Since the split wedge is a two-piece wedge type, it has been observed that the pressure is high at the junction points of the pieces. It is observed that the speed increases with the decrease in pressure, especially at the wedge tip.

Figure 9 shows the pressure distributions of 60 mm wedge opening and 4 degrees wedge closing angle. It is understood that the pressure at the tip of the wedge is higher than the 20 mm and 40 mm opening positions, and the pressure distribution is higher at the split wedge output section than the solid and flexible wedge types. With the flow velocity increasing from 0.5 m/s to 2 m/s for the 60

Type	0.5 m/s Flow rate	1 m/s Flow rate	2 m/s Flow rate
Flexible	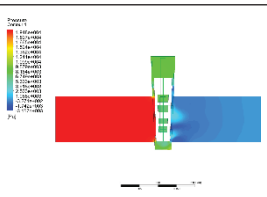	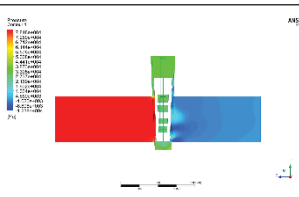	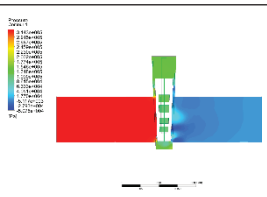
Solid	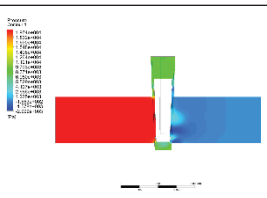	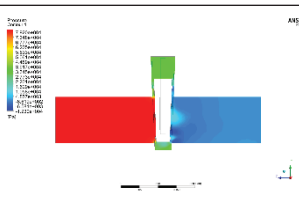	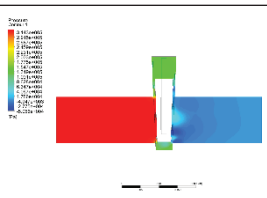
Split	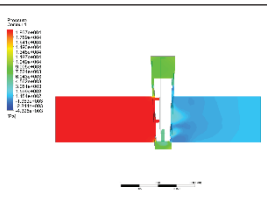	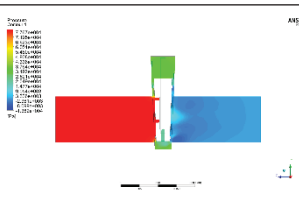	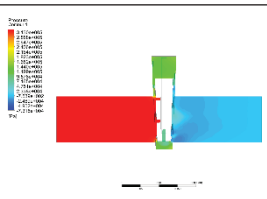

Figure 7. 20 mm wedge opening and 4-degree wedge close angle pressure distribution.

Type	0.5 m/s Flow rate	1 m/s Flow rate	2 m/s Flow rate
Flexible	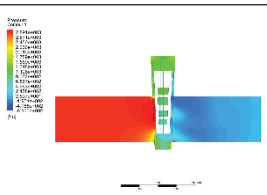	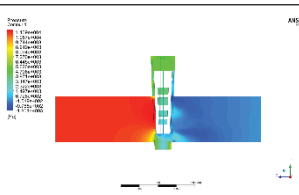	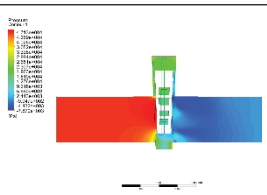
Solid	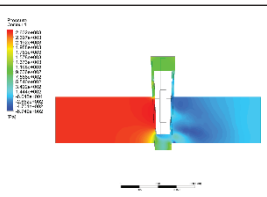	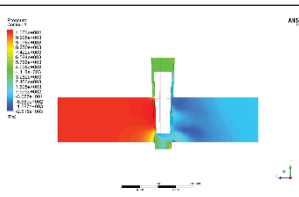	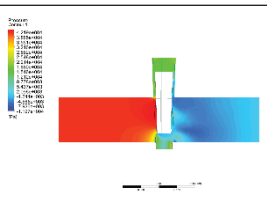
Split	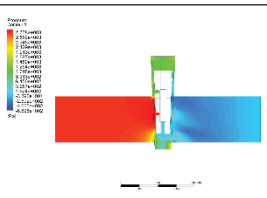	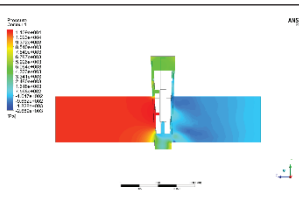	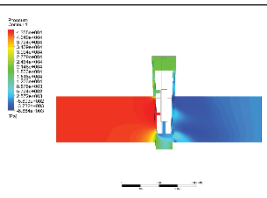

Figure 8. 40 mm wedge opening and 4-degree wedge close angle pressure distribution.

mm wedge opening, the maximum pressure formed due to the analysis increased approximately 17.4, 16.2, and 12 times for flexible, solid, and split wedge types, respectively. Since the split wedge is a two-piece wedge type, it has been observed that the pressure is high at the junction points of the pieces. It is observed that the speed increases with the decrease in pressure, especially at the wedge tip.

Figure 10 shows pressure distributions according to 90 mm wedge opening and 4 degrees wedge closing angle. At the flexible wedge, it can be seen that the pressure is maximum for all flow rates. This means that this type of wedge cuts the flow. In the solid wedge type, it was seen that the flow was compressed in the upper part of the wedge, and there is a homogeneous pressure distribution in the other areas. For the split wedge, it is seen that the pressure distribution is homogeneously distributed at low speeds, but the pressure in the inlet section increases with the increase of the flow rate. It has been observed that with the increase of the flow velocity from 0.5 m/s to 2 m/s for 90 mm wedge opening, pressure occurs especially at the wedge tip of the flexible wedge type.

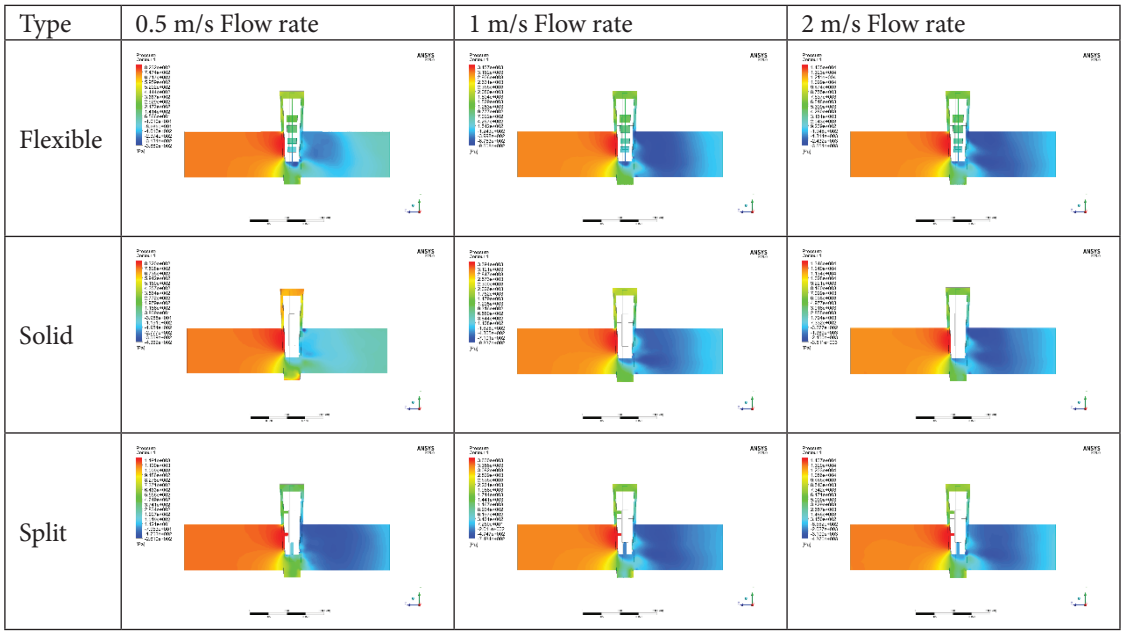

Figure 9. 60 mm wedge opening and 4-degree wedge close angle pressure distribution.

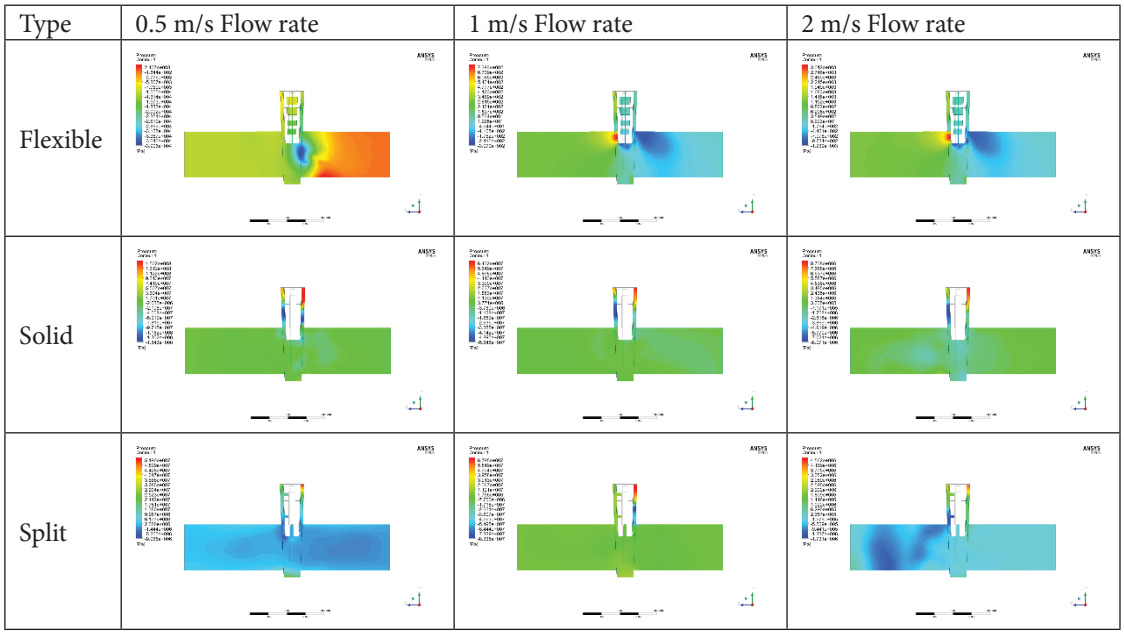

Figure 10. 90 mm wedge opening and 4-degree wedge close angle pressure distribution.

In addition, in solid and split wedge types, it is seen that the pressure towards the wedge slot increases with the increase in flow velocity. Pressure build-up towards this slot will cause deterioration in the parts that provide the wedge movement and the wedge slot over time.

Figure 11 shows pressure distributions of 120 mm wedge opening and 4 degrees wedge closing angle. It is seen that regional pressure differences occur for the flexible wedge and this decreases especially with the increase in flow rate. It can be said that the maximum pressure is the lowest for the split wedge type, and it is the type that affects the least in terms of pressure loss. It has been observed that with the increase of the flow velocity from 0.5 m/s to 2 m/s for 120 mm wedge opening, pressure occurs especially at the wedge tip of the flexible wedge type. In addition, in solid and split wedge types, it is seen that the pressure towards the wedge slot increases with the increase in flow velocity. Pressure build-up towards this slot will cause deterioration in the parts that provide the wedge movement and the wedge slot over time. In particular, the reason for the

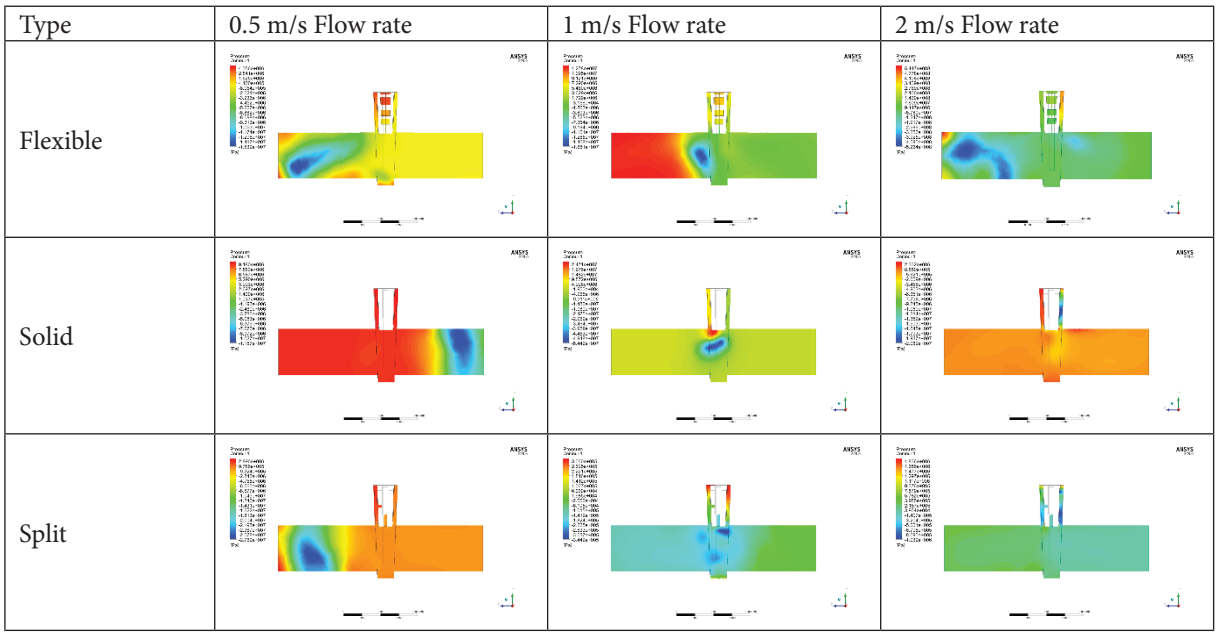

Figure 11. 120 mm wedge opening and 4-degree wedge close angle pressure distribution.

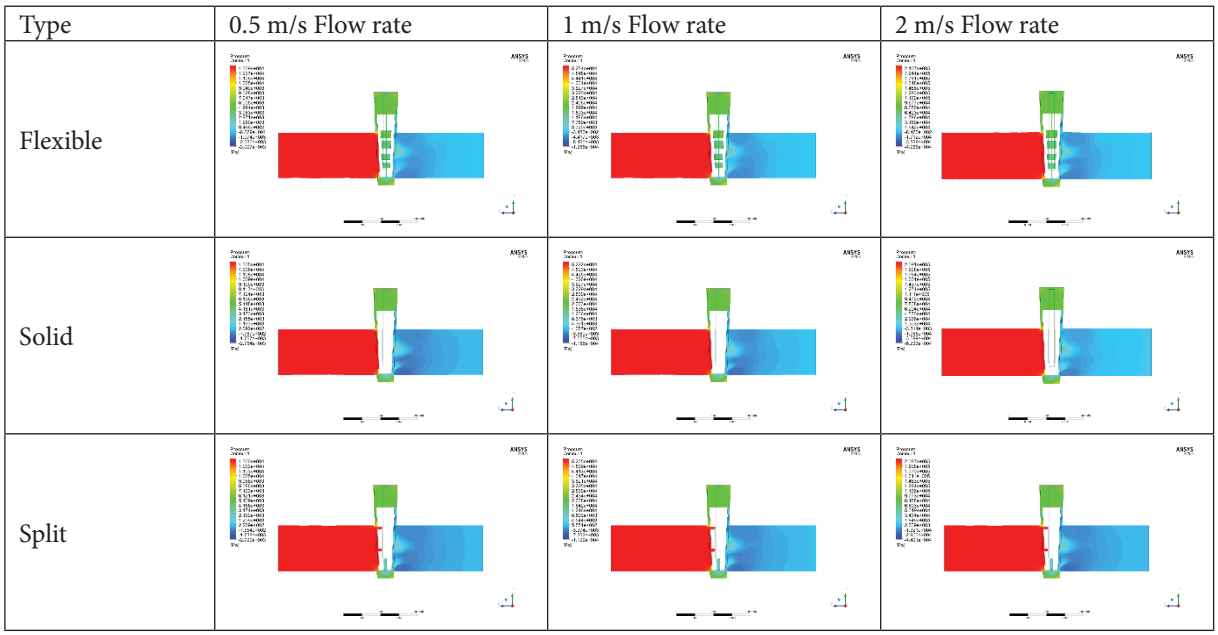

Figure 12. 20 mm wedge opening and 5-degree wedge close angle pressure distribution.

regional deterioration of the pressure distribution is that the flow enters the wedge slot and with its effect, the flow has changed regionally in the analysis.

Figure 12 shows the pressure distributions of 20 mm wedge opening and 5 degrees wedge closing angle. In general, it is understood that the pressure in the inlet part is higher than in the outlet part. Especially when looking at the split wedge, it can be said that there is more pressure in the middle of the wedge than in other types of wedges, which may cause pressure loss in the flow and the wedge should be specially coated since it is exposed to drag pressure for the wedge. It is seen that a split wedge is formed for a maximum regional pressure of 0.21 MPa and a flow rate of 2 m/s. It can be said that the maximum pressures are lower at the 20 mm opening position compared to the 4-degree wedge closing angle. This situation can be expressed as less pressure loss.

Figure 13 shows pressure distributions of 40 mm wedge opening and 5 degrees wedge closing angle. In general, it is understood that the pressure is higher in the inlet part of the gate valve and the pressure is lower in the outlet part.

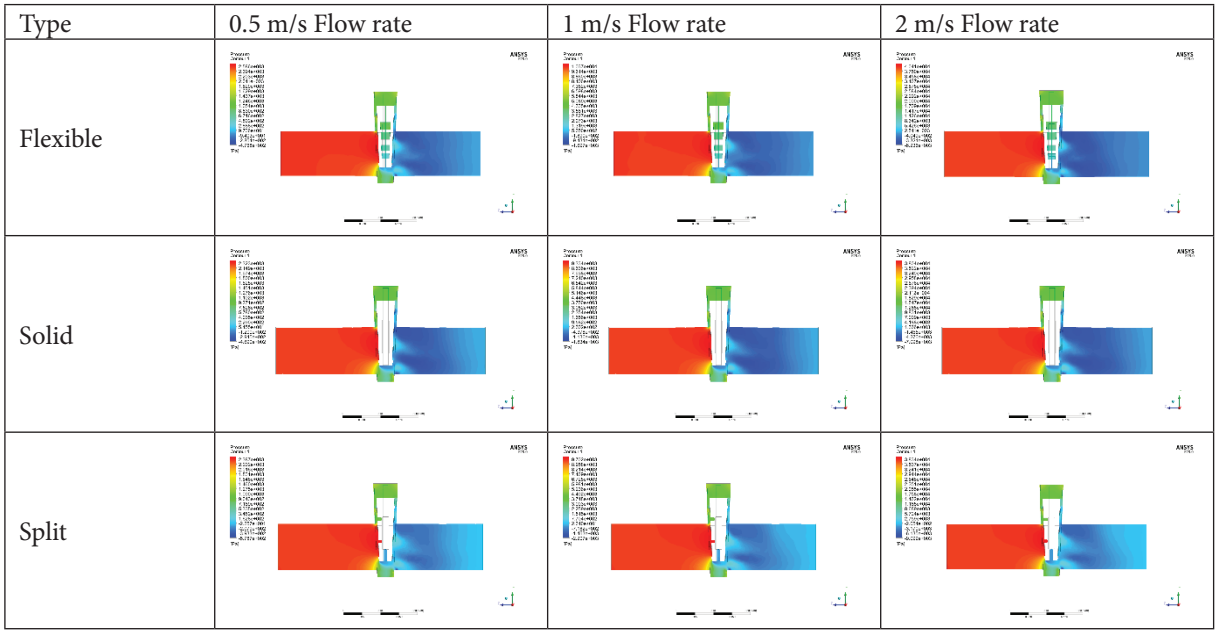

Figure 13. 40 mm wedge opening and 5-degree wedge close angle pressure distribution.

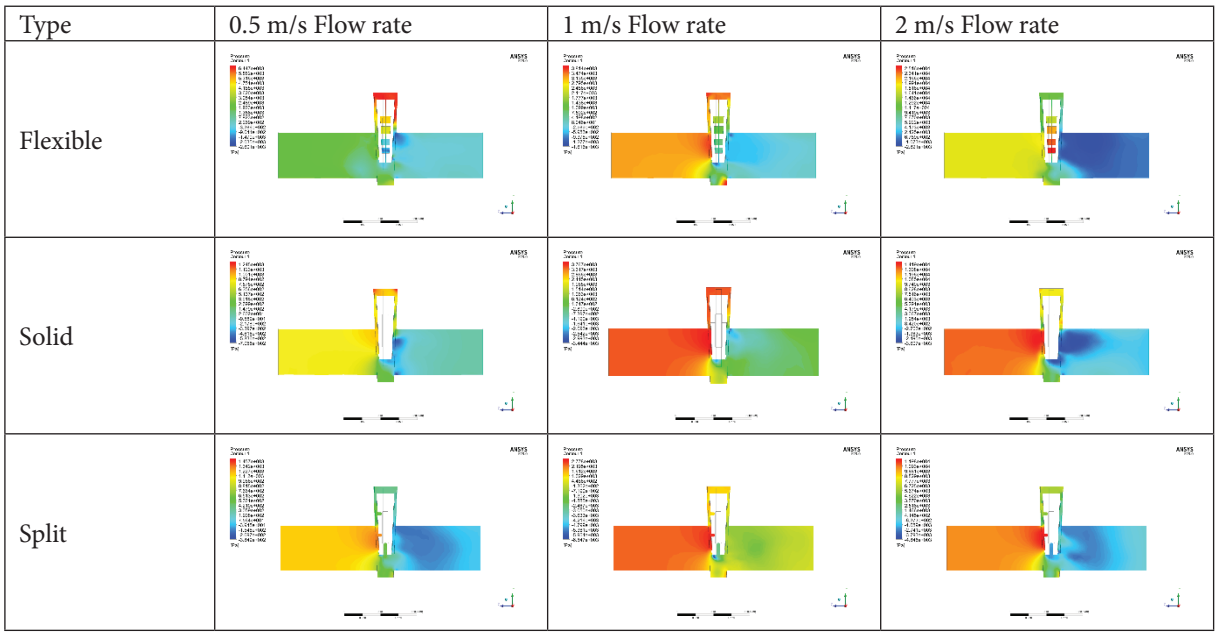

Figure 14. 60 mm wedge opening and 5-degree wedge close angle pressure distribution.

Especially when looking at the split wedge, it can be said that there is more pressure in the middle of the wedge than in other types of wedges, which may cause pressure loss in the flow and the wedge should be specially coated since it is exposed to drag pressure for the wedge. It is seen that a flexible wedge is formed for maximum regional pressure of 0.04 MPa and a flow rate of 2 m/s. It can be said that the maximum pressures are lower at the 40 mm opening position compared to the 4-degree wedge closing angle. This can be expressed as less pressure loss.

Figure 14 shows pressure distributions according to 60 mm wedge opening and 5 degrees wedge closing angle. In general, it is seen that the pressure difference in the inlet and outlet parts begins to decrease. When looking at the split wedge, it can be said that there is more pressure in the middle of the wedge than other wedge types, which may cause pressure loss in the flow and the wedge may be subject to wear because it is exposed to drag pressure for the wedge. It is seen that a flexible wedge is formed for a maximum regional pressure of 0.025 MPa and a flow rate of 2 m/s.

Figure 15 shows the pressure distributions according to the 90 mm wedge opening and the 5-degree wedge closing angle. In general, it is seen that the pressure difference in the inlet and outlet parts is almost non-existent. When looking at the split wedge, it is seen that there is a higher pressure at the tip of the wedge for 1 m/s and 2 m/s flow velocities compared to other wedge types. It can be said that the pressure distribution is homogeneous for a flow velocity of 0.5 m/s for the solid wedge type. It is seen that 607 MPa regional maximum pressure occurs in the split wedge for 0.5 m/s flow velocity. The increase in regional pressure on the upper part of the wedge means that this region is a risky point. Gate valve-type valves are not used as proportional valves, and it can be said that it is necessary to open the valve very quickly to prevent scour in this area when opening the valve.

Figure 16 shows the pressure distributions of the 120 mm wedge opening and the 5-degree wedge closing angle. In general, it is seen that the pressure difference in the inlet and outlet parts is almost non-existent. When looking at the split wedge, it is seen that there is a higher pressure at the tip of the wedge for 1 m/s and 2 m/s flow velocities compared to other wedge types. It can be said that the pressure distribution is homogeneous for a flow velocity of 0.5 m/s for the solid wedge type. It is seen that 607 MPa regional maximum pressure occurs in the split wedge for 0.5 m/s flow velocity. The increase in regional pressure on the upper part of the wedge means that this region is a risky point. Gate valve-type valves are not used as proportional valves, and it can be said that it is necessary to open the valve very quickly to prevent scour in this area when opening the valve [43].

Figure 17 shows the analysis results for different flow rates and wedge opening positions for the parallel wedge. It can be said that as the gate opening increases, the pressure of the inlet and outlet region is equalized. As the flow rate increases, the pressure values also increase. For 20 mm and 40 mm wedge openings, high maximum pressure values occur due to the small wedge opening even at low speeds. If the wedge opening is at 60 and 90 mm, it is seen that pressure builds up at the tip of the wedge with the effect of the flow. At 120 mm, however, since the wedge is pulled inwards, the flow towards this region creates a pressure on the wedge

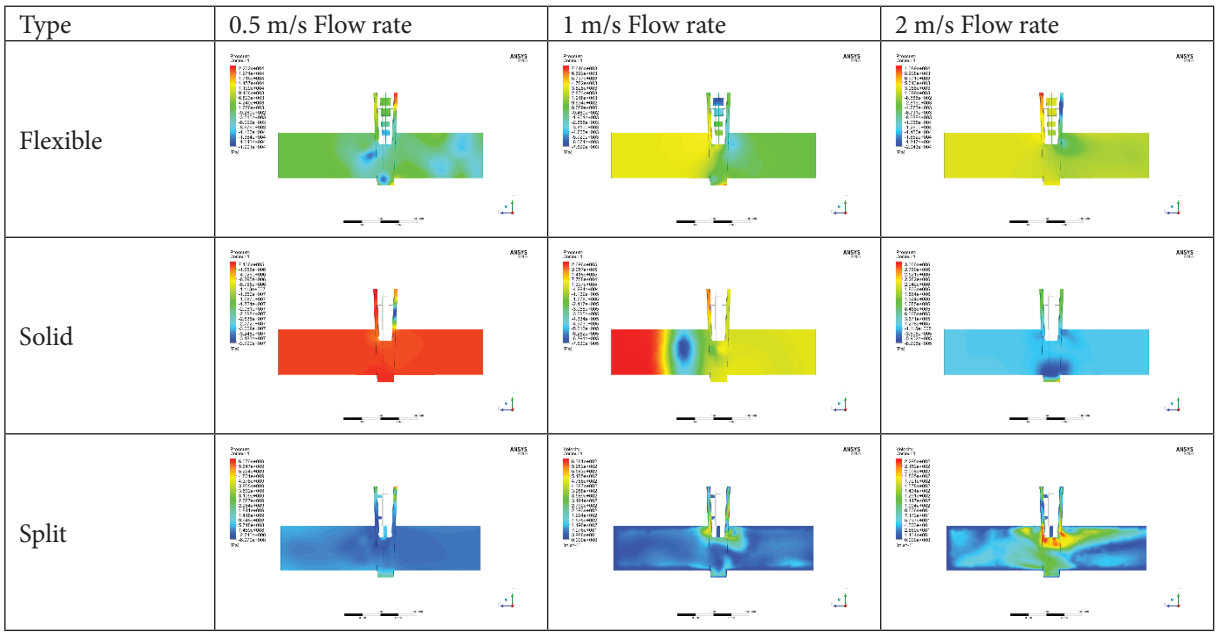

Figure 15. 90 mm wedge opening and 5-degree wedge close angle pressure distribution.

Type	0.5 m/s Flow rate	1 m/s Flow rate	2 m/s Flow rate
Flexible	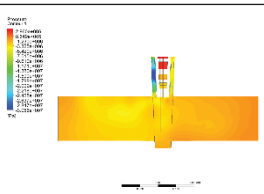	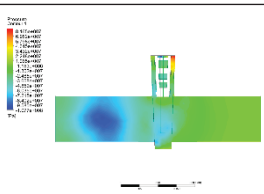	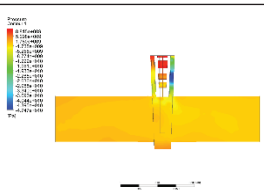
Solid	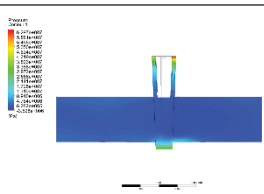	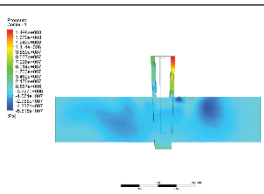	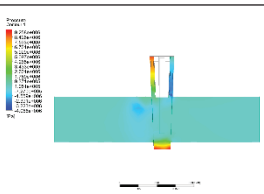
Split	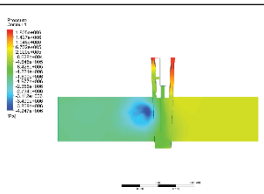	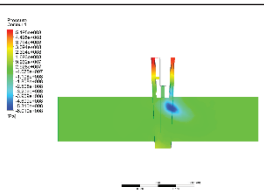	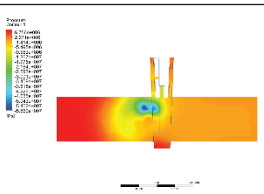

Figure 16. 120 mm wedge opening and 5-degree wedge close angle pressure distribution.

Lift	0.5 m/s Flow rate	1 m/s Flow rate	2 m/s Flow rate
20 mm	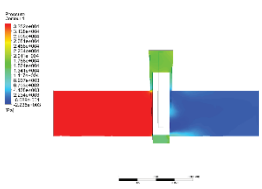	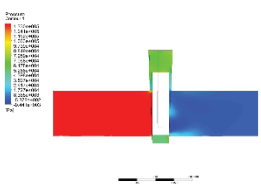	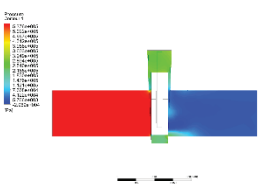
40 mm	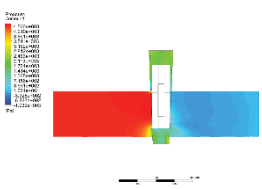	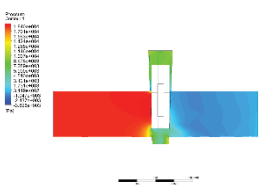	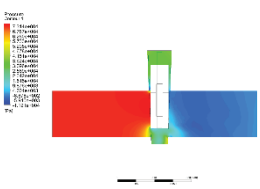
60 mm	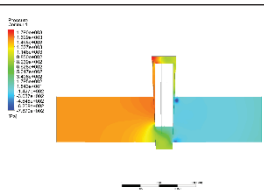	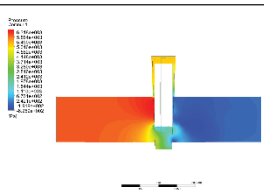	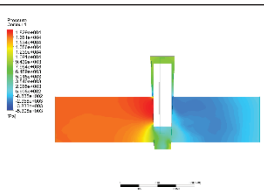
90 mm	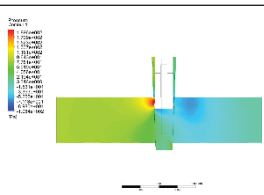	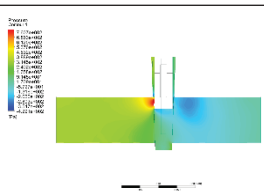	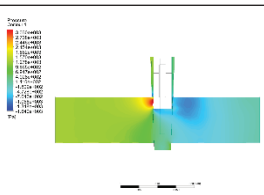
120 mm	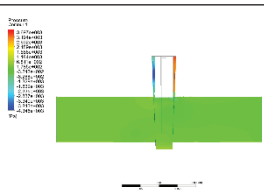	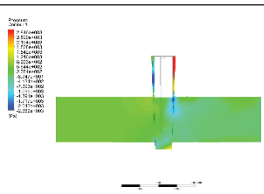	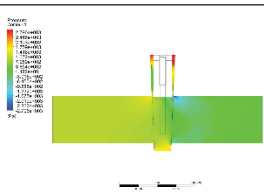

Figure 17. Parallel wedge opening and 0-degree wedge close angle pressure distribution.

surface inside. As the flow rate increases, this pressure effect increases. Especially at 60 and 90 mm wedge opening position, it is thought that scours will be caused by the effect of flow at the wedge end. It is seen that the gate at the 90 mm opening affects the flow. It can be stated that the wear of the valve in this opening will be too much. With the flow velocity increasing from 0.5 m/s to 2 m/s for 20 mm and 40 mm wedge opening, the maximum pressure generated as a result of the analysis increased approximately 16 times. Likewise, for the 60 mm wedge opening, the maximum pressure increased 10.2 times with the increase of the speed by 4 times. At 90 and 120 mm, there was a difference in maximum pressure of 15.9 times, similar to 20 and 40 mm openings [44].

Experimental Results

Another study, the study in which the wedge angle is 0 degrees, has been studied for the same parameters and its difference from other types of wedge designs will be interpreted here. Figure 17 shows the variation of parallel wedge-type pressure distributions according to the wedge opening position. It has been observed that it cuts the flow less and is exposed to less pressure than other wedge types. For this reason, it has been seen that it is more suitable for Gate valve types at 2 m/s flow rates compared to other wedge types.

Leakage test times of the metal gate valve and soft gate valve were observed by adhering to the tests performed at every 100 opening-closing times. Leakage amounts are given in Table 1 according to the number of tests performed. The metal gate valve gave four bubble leakage in test no. 19. As the number of tests increased, the amount of leakage started to increase. On the other hand, the soft seat gate valve started to leak in the 41st test. While the metal sealing valve gives an 1800 opening-closing life, this amount has increased to 4000 opening-closing amount with the soft seat gate valve design. It has been observed that the metal gate valve gives an average of 10 times leakage compared to the soft seat gate valve in the number of tests where two valves leak at the same time. This improvement has achieved a delay in sealing time of approximately 2.5 times. Tightness test results for the designated gate valve are in Table 2.

Table 2. Comparison of soft seat gate valve and metal seat gate valve test results

TEST NUMBER	SOFT SEAT GATE VALVE (SIZE: 8”)	METAL SEAT GATE VALVE (SIZE: 8”)	TEST NUMBER	SOFT SEAT GATE VALVE (SIZE: 8”)	METAL SEAT GATE VALVE (SIZE: 8”)
	Water (bubbles per minute)	Water (bubbles per minute)		Water (bubbles per minute)	Water (bubbles per minute)
1	0	0	23	0	6
2	0	0	24	0	6
3	0	0	25	0	9
4	0	0	26	0	11
5	0	0	27	0	12
6	0	0	28	0	12
7	0	0	29	0	12
8	0	0	30	0	12
9	0	0	31	0	14
10	0	0	32	0	14
11	0	0	33	0	14
12	0	0	34	0	14
13	0	0	35	0	15
14	0	0	36	0	18
15	0	0	37	0	18
16	0	0	38	0	24
17	0	0	39	0	24
18	0	0	40	0	33
19	0	4	41	4	40
20	0	4	42	4	44
21	0	6	43	6	51
22	0	6	44	6	54

1 Millilitre = 16 drops ; 1 Millilitre = 7 bubbles

*** ISO 5208 or ANSI/FCI 70 leakage rates can also be specified.**

CONCLUSION

Analyzes were performed for different wedge closing angles and open positions. As a result of the analyzes made, the following evaluations were obtained. The experimental study was carried out for parallel wedge-type gate valves according to the analysis results. Teflon coating has also been applied to increase the sealing and life of this valve.

It has been observed that the highest maximum pressures are obtained at the wedge 120 mm opening positions compared to

1. Wedge open positions and the maximum pressures are lower at low wedge openings.
2. It has been observed that a lower maximum pressure occurs with a wedge closing opening of 5 degrees compared to a wedge closing opening of 4 degrees. It is seen that 4 degrees wedge closure angle is more suitable for low fluid velocity, but 5 degrees wedge closure angle causes lower maximum pressure with increasing fluid velocity.
3. In the case of the parallel wedge, that is, the wedge closing angle of 0 degrees, it is seen in the analysis results that the maximum pressure formation is lower. For this reason, it is recommended that the parallel wedge type can be used for a maximum fluid velocity of 2 m/s, especially in gate valves, depending on the fluid velocity and different opening positions.

The 4-Gate valve type, especially the parallel wedge type is suitable for flow rates up to 2 m/s.

Especially since the gate valve requires designs specific to the sector and area in which it will be used, this study has been done considering that it will help the parameters in selecting wedge type for the design. This study presents wedge types and their effects on flow visually.

The Teflon-reinforced sealing surface, created in gate valves to extend the sealing life and ensure the performance at the same pressure values, has achieved complete success after the tests. The Teflon ring on the gate surface provides both higher performance and longer sealing life in processes exposed to corrosion, especially since its corrosion resistance is superior to steel materials. Pressure loss occurs due to the operating principles of the valves on the line. Line cleaning operations on the valves are only possible with full-bore valves. Made by the PIG method, uninterrupted and fast cleaning of the line in cleaning increases the efficiency of line usage. In tank farms, independent liquids are transferred after cleaning the same line. In particular, the storage is connected to the lines where multiple fluids are transported. In case of internal leakage in the tanks, there is a risk of mixing different liquids. It has been observed that the rate of internal leakage increases in the formation of high friction force and wear on the gate, especially at high opening and closing numbers. The friction of metal with Teflon. As a result, it was observed that the wear occurred later than the metal surface.

It can be said that the soft seat gate valve, which is designed according to the results of the sealing test, gives approximately 2.5 times more opening-closing life than the metal gate valve, thus reducing the maintenance-repair costs.

ACKNOWLEDGMENTS

This work was supported by Kocaeli University Scientific Research Projects Coordination Unit. Project Number: FDK-2021-2454

AUTHORSHIP CONTRIBUTIONS

Authors equally contributed to this work.

DATA AVAILABILITY STATEMENT

The authors confirm that the data that supports the findings of this study are available within the article. Raw data that support the finding of this study are available from the corresponding author, upon reasonable request.

CONFLICT OF INTEREST

The author declared no potential conflicts of interest with respect to the research, authorship, and/or publication of this article.

ETHICS

There are no ethical issues with the publication of this manuscript.

REFERENCES

[1] Weibel DB, Kruithof M, Potenta S, Sia SK, Lee A, Whitesides GM. Torque-actuated valves for microfluidics. Anal Chem 2005;77:4726-4733. [CrossRef]

[2] Tabrizi AS, Asadi M, Xie G, Lorenzini G, Biserni C. Computational fluid-dynamics-based analysis of a ball valve performance in the presence of cavitation. J Engineer Thermophys 2014;23:27-38. [CrossRef]

[3] Manahan GJ. Gate valve design and application. Sewage Ind Wastes 1956;28:225-231.

[4] Wheeler WR. Recent developments in metal-sealed gate valves. J Vac Sci Technol 1998;13:503-506. [CrossRef]

[5] Aslanov JN, Mammadov KS. Design and performance analysis of improved valve construction being used in oil and gas industry. Int J Tech Phys Probl Engineer 2022;14:98-103.

[6] Larsen CG, Johnson LE, Mosiman LG. Gripping techniques and concerns for mechanical testing of ultra-high temperature materials. Ultra High Temp Mech Test 1995:35-50. [CrossRef]

[7] Panciroli R, Abrate S, Minak G. Dynamic response of flexible wedges entering the water. Compos Struct 2013;99:163-171. [CrossRef]
[8] Anderson CN, Bosserman BE, Morris CD, Cadrecha C, Lescovich JE, Taylor HW, et al. Valves. In: Jones GM, Sanks RL, Tchobanoglous G, Bosserman BE, eds. Pumping Station Design. Oxford: Butterworth-Heinemann; 2008. [CrossRef]
[9] Tverskoy MM, Andrianov VN, Sokolov AV. Creating new generation of actuators for shut-off and control ball valves with double-gate. Procedia Engineer 2017;206:1303-1308. [CrossRef]
[10] Zakirnichnaya MM, Kulsharipov IM. Wedge gate valves selected during technological pipeline systems designing service life assessment. Procedia Engineer 2017;206:1831-1838. [CrossRef]
[11] Bakic G, Zeravcic VS, Djukic MB, Perunicic V, Prodanovic A, Rajicic B, et al. Material characterization of the main steam gate valve made of X20CrMoV 12.1 steel after long term service. Procedia Mater Sci 2014;3:1512-1517. [CrossRef]
[12] Tripathy S, Das A, Sahu B, Srivastava DK. Electro-pneumatic variable valve actuation system for camless engine: Part I-development and characterization. Energy 2020;193:116740. [CrossRef]
[13] Battini D, Donzella G, Avanzini A, Zenoni A, Ferrari M, Donzella A, et al. Experimental testing and numerical simulations for life prediction of gate valve O-rings exposed to mixed neutron and gamma fields. Mater Des 2018;156:514-527. [CrossRef]
[14] Kim DW, Park SG, Kang SC, Kim YS. A study on the phenomenon of rate of loading in motor operated gate valves. Nucl Engineer Des 2010;240:957-962. [CrossRef]
[15] Kim DW, Park SG, Lee SG, Kang SC. A study on a characteristic of stem friction coefficient for motor operated flexible wedge gate valve. Nucl Engineer Des 2009;239:1744-1749. [CrossRef]
[16] Teodoro OMND, Moutinho AMC. Compact gate valve for UHV. Vacuum 2001;64:87-90. [CrossRef]
[17] Qian J, Liu B, Lei L, Zhang H, Lu A, Wang JK, et al. Effects of orifice on pressure difference in pilot-control globe valve by experimental and numerical methods. Int J Hydrogen Energy 2016;41:18562-18570. [CrossRef]
[18] Qian J, Gao Z, Wang JK, Jin ZJ. Experimental and numerical analysis of spring stiffness on flow and valve core movement in pilot control globe valve. Int J Hydrogen Energy 2017;42:17192-171201. [CrossRef]
[19] Qian J, Wei L, Jin ZJ, Wang JK, Zhang H, Lu AL. CFD analysis on the dynamic flow characteristics of the pilot-control globe valve. Energy Conver Manage 2014;87:220-226. [CrossRef]
[20] Alimonti C. Experimental characterization of globe and gate valves in vertical gas-liquid flows. Exp Therm Fluid Sci 2014;54:259-266. [CrossRef]
[21] Paolinelli LD, Rashedi A, Yao J. Characterization of droplet sizes in large scale oil-water flow downstream from a globe valve. Int J Multiph Flow 2018;99:132-150. [CrossRef]
[22] Prakash AS, Ram KS. Aeroacoustics analysis of globe control valves. Int J Automot Mech Engineer 2018;15:5547-5561. [CrossRef]
[23] Mitrovic N, Petrovic A, Milosevic M, Momcilovic N, Miskovic Z, Maneski T, et al. Experimental and numerical study of globe valve housing. Hem Ind 2017;71:251-257. [CrossRef]
[24] Ferrari JL. Measurement of the fluid flow load on a globe valve stem under various cavitation conditions. Available at: https://arxiv.org/abs/0909.0874. Accessed Aug 20, 2024.
[25] Azam FI, Rani AMA, Altaf K, Zaharin HA. Experimental and numerical investigation of six-bar linkage application to bellow globe valve for compact design. Appl Sci 2018;8:1980. [CrossRef]
[26] Lin Z, Sun X, Yu T, Zhang Y, Li Y, Zhu Z. Gas-solid two-phase flow and erosion calculation of gate valve based on the CFD-DEM model. Powder Technol 2020;366:395-407. [CrossRef]
[27] Hu B, Zhu H, Ding K, Zhang Y, Yin B. Numerical investigation of conjugate heat transfer of an underwater gate valve assembly. Appl Ocean Res 2016;56:1-11. [CrossRef]
[28] Borooghani B, Ashrafi A, Valeh H, Honarvar H. Failure analysis of a gate valve bonnet at wellhead facilities in sour gas service. Engineer Fail Anal 2020;108:104250. [CrossRef]
[29] Farsi C, Amroune S, Moussaoui M, Mohamad B, Benkherbache H. High-gradient magnetic separation method for weakly magnetic particles: An industrial application. Metallofiz Nov Tekhnol 2019;41:1103-1119. [CrossRef]
[30] Amroune S, Belaadi A, Menasri N, Zaoui M, Mohamad B, Amin H. New approach for computer-aided static balancing of turbines rotors. Diagnostyka 2019;20:95-101. [CrossRef]
[31] Benkherbache H, Amroune S, Zaoui M, Menaseri N, Mohamad B, Silem M, et al. Characterization and mechanical behaviour of similar and dissimilar parts joined by rotary friction welding. Engineer Solid Mech 2020;9:23-30. [CrossRef]
[32] Amroune S, Belaadi A, Zaoui M, Menasri N, Mohamad B, Saada K, et al. Manufacturing of rapid prototypes of mechanical parts using reverse engineering and 3D printing. J Serbian Soc Comput Mech 2021;15:167-176. [CrossRef]
[33] Sai Chandra A, Nithish Reddy P, Kasaeian A. Natural ventilation in a large space with heat source: CFD visualization and taguchi optimization. J Therm Engineer 2022;8:642-655. [CrossRef]
[34] Azeez K, Rahim A, Talib A, Ahmed RI, Kılıç M. Heat transfer enhancement for corrugated facing

step channels using aluminium nitride nanofluid - Numerical investigation. J Therm Engineer 2022;8:734-747. [CrossRef]

[35] Taskesen E, Tekir M, Gedik E, Arslan K. Numerical investigation of laminar forced convection and entropy generation of Fe3O4/water nanofluids in different cross-sectioned channel geometries. J Therm Engineer 2021;7:1752-1767. [CrossRef]

[36] Berkache A, Boumehani A, Noura B, Kerfah R. Numerical investigation of 3D unsteady flow around a rotor of vertical axis wind turbine darrieus type H. J Therm Engineer 2022;8:691-701. [CrossRef]

[37] Parkash O, Arora R. Flow characterization of multi-phase particulate slurry in thermal power plants using computational fluid dynamics. J Therm Engineer 2020;6:187-203. [CrossRef]

[38] Abay K, Colak U, Yüksek L. Computational fluid dynamics analysis of flow and combustion of a diesel engine. J Therm Engineer 2017;4:1878-1895. [CrossRef]

[39] Badra J, Viollet Y, Elwardany A, Im HG, Chang J. Physical and chemical effects of low octane gasoline fuels on compression ignition combustion. Appl Energy 2016;183:1197-1208. [CrossRef]

[40] Ahmed SU, Arora R, Parkash O. Numerical investigations on flow characteristics of sand-water slurry through horizontal pipeline using computational fluid dynamics. J Therm Engineer 2020;6:140-151. [CrossRef]

[41] Selimli S, Dumrul H, Yilmaz S, Akman O. Experimental and numerical analysis of energy and exergy performance of photovoltaic thermal water collectors. Sol Energy 2021;228:1-11. [CrossRef]

[42] Moussa O, Driss Z. Numerical investigation of the turbulence models effect on the combustion characteristics in a non-premixed turbulent flame methane-air. Am J Energy Res 2017;5:85-93.

[43] Wu H, Li JY, Gao Z. Flow characteristics and stress analysis of a parallel gate valve. Process 2019;7:803. [CrossRef]

[44] Žic E, Banko P, Lešnik L. Hydraulic analysis of gate valve using computational fluid dynamics (CFD). Sci Rev Engineer Environ Stud 2020;29:275-288. [CrossRef]